JOC The Journal of Organic Chemistry

Article

Svetamycins A-G, Unusual Piperazic Acid-Containing Peptides from Streptomyces sp.

Denis Dardic, Gianluigi Lauro, Giuseppe Bifulco, Patricia Laboudie, Peyman Sakhaii, Armin Bauer, Andreas Vilcinskas, Peter E. Hammann, and Alberto Plaza

J. Org. Chem., **Just Accepted Manuscript** • Publication Date (Web): 10 May 2017

Just Accepted

ACS Publications

The Journal of Organic Chemistry is published by the American Chemical Society.
1155 Sixteenth Street N.W., Washington, DC 20036

Svetamycins A-G, Unusual Piperazic Acid-Containing Peptides from *Streptomyces* sp.

Denis Dardić,[†] *Gianluigi Lauro*[‡] *Giuseppe Bifulco,*[‡] *Patricia Laboudie,*[ǀ] *Peyman Sakhaii,*[§] *Armin Bauer,*[⊥] *Andreas Vilcinskas,*[†] *Peter E. Hammann,*[⊥] *Alberto Plaza**[,†,±]

[†] Sanofi-Fraunhofer Natural Product Center of Excellence, Fraunhofer IME, Industriepark Höchst Bldg. G878, 65926, Frankfurt am Main, Germany

[‡] Dipartimento di Farmacia, Università di Salerno, Via Giovanni Paolo II 132, 84084 Fisciano (SA), Italy

[ǀ] Infectious Diseases Therapeutic Area, Sanofi R&D, Campus Mérieux, 1541 avenue Marcel Mérieux, XNord 315, 69280 Marcy L'Etoile, France

[§] NMR Laboratory, Chemistry & Biotechnology Development Frankfurt Chemistry, Sanofi-Aventis Deutschland GmbH, Industriepark Hoechst, Bldg. G849, 65926, Frankfurt am Main, Germany.

[⊥] R&D Infectious Diseases Therapeutic Area, Sanofi-Aventis Deutschland GmbH, Industriepark Höchst Bldg. G878, 65926, Frankfurt am Main, Germany

*E-mail: Alberto.Plaza@merckgroup.com

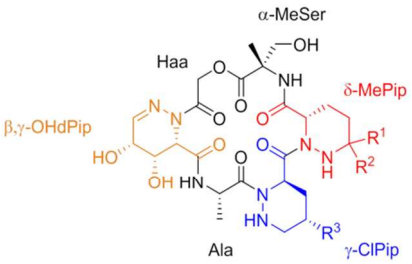

Svetamycin A	$R^1 = R^2 = H$	$R^3 = Cl$
Svetamycin C	$R^1 = R^2 = Me$	$R^3 = Cl$
Svetamycin I	$R^1 = R^2 = Me$	$R^3 = Br$

ABSTRACT

Seven new halogenated peptides termed svetamycins A-G (**1-7**) have been isolated from laboratory cultures of a *Streptomyces* sp. Svetamycins A-D, F, and G are cyclic depsipeptides whereas svetamycin E is a linear analogue of svetamycin C. Their structures were determined using extensive spectroscopic analysis, and their stereochemical configuration was established by a combination of NMR data, quantum mechanical calculations, and chemical derivatizations. Svetamycins are characterized by the presence of a hydroxyl acetic acid and five amino acids including a rare 4,5-dihydroxy-2,3,4,5-tetrahydropyridazine-3-carboxylic acid, a γ-halogenated piperazic acid, and a novel δ-methylated piperazic acid in svetamycins B-C, E, and G. Moreover, isotope-labeled substrate feeding experiments demonstrated ornithine as the precursor of piperazic acid and that methylation at the δ position of the piperazyl scaffold is *S*-adenosyl-L-methionine (SAM)-dependent. Svetamycin G, the most potent antimicrobial of this suite of compounds, inhibited the growth of *Mycobacterium smegmatis* with an MIC_{80} value of 2 μg/mL.

INTRODUCTION

The emergence of resistance to antibiotics is unavoidable due to the natural selection for resistant pathogens that takes place with each generation of newly discovered antibiotics.[1] Therefore, there is a continuous need to identify new lead antimicrobials with improved activities and/or novel mechanisms of action. Microorganisms are an excellent source of new antimicrobial natural products skeletons because of their capability to synthesize a plethora of small molecules with fascinating chemical structures and potent biological properties. Indeed, four antibacterial small molecules approved by the U.S. FDA during 2011 to 2014 were either microbial derived-natural products or synthetic derivatives thereof.[2] As part of an ongoing collaboration between Fraunhofer IME and Sanofi, we have screened a part of the Sanofi's microbial extract library for antibacterial activity against opportunistic microbial pathogens. In particular, methanol extracts of a *Streptomyces* sp. (DSM 14386) strongly inhibited the growth of *Eschericia coli*, MRSA, and *Mycobacterium smegmatis*. Bioassay and UPLC-HRMS-guided fractionation led to the isolation of five new chlorinated peptides termed svetamycins A-E (**1**-**5**) together with the known chlorinated pentalenolactone AA-57.[3] Additionally, to determine if strain DSM 14386 was biosynthetically capable of producing other halogenated peptides, DSM 14386 was cultivated with a nutrient medium supplemented with sodium bromide leading to the production of two brominated congeners named svetamycin F (**6**) and G (**7**). Their structures were elucidated by extensive NMR and HR-ESI-MS analysis along with quantum mechanical calculations, chemical derivatization, and circular dichroism experiments.

RESULTS AND DISCUSSION

Large scale fermentation (20 L) of DSM14386 was carried out, and the culture supernatant was treated with a mixture of Amberlite® XAD-7 and -16. The bound compounds were extracted with methanol and the dried extract was fractionated by Sephadex LH-20 column chromatography, and further subjected to semi preparative HPLC (C-12 column) to yield pure compounds **1**−**5**. An additional fermentation was conducted on agar plates in which the NaCl of the fermentation media was replaced with an equal amount of NaBr. Accordingly, fractionation of the generated methanol extracts afforded the brominated compounds **6** and **7**.

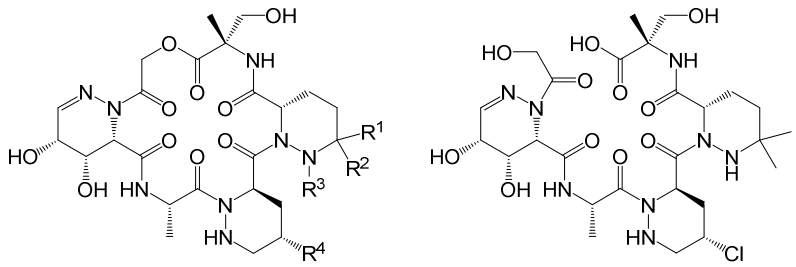

1	R^1=R^2=R^3=H	R_4 = Cl
2	R^1=H, R^2=Me, R^3=H	R_4 = Cl
3	R^1=R^2=Me, R^3=H	R_4 = Cl
4	R^1=H, R^2-R^3=π-bond	R_4 = Cl
6	R^1=R^2=R^3=H	R_4 = Br
7	R^1=R^2=Me, R^3=H	R_4 = Br

5

The most abundant compound among this group was svetamycin A (**1**). Its molecular formula was determined as $C_{24}H_{35}ClN_8O_{10}$ based on HR-ESI-MS and NMR data (see Table 1), indicating 11 degrees of unsaturation. The HSQC spectrum of **1** exhibited resonances characteristic of a peptide bearing oxygenated and imine functionalities including four α-amino methines (δ_H 4.90, δ_c 50.9; δ_H 5.73, δ_c 49.8; δ_H 5.33, δ_c 43.1; δ_H 4.71, δ_c 56.9), two oxymethines (δ_H 3.93, δ_c 62.6; δ_H 4.06, δ_c 63.8), two oxymethylene (δ_H 3.67, 3.82, δ_c 63.6;. δ_H 4.64, 5.30, δ_c 61.5), and one olefinic methine (δ_H 6.97, δ_c 147.2). Besides, the ^{13}C NMR spectrum showed resonances ascribable to six carbonyls at δ 166.6 - 172.7 and one quaternary carbon at δ 60.4. Further analysis of the 2D

NMR data allowed us to determine the presence of the amino acids alanine, α-methlyserine (α-MeSer), piperazic acid (Pip), and γ-chloro-piperazic acid (γ-ClPip) together with a hydroxyacetic acid residue (Haa). Additionally, TOCSY and COSY spectra showed that the remaining spin system comprised an imine proton (H-$5_{\beta,\gamma\text{-OHdPip}}$) two oxymethines (H-$3_{\beta,\gamma\text{-OHdPip}}$ and H-$4_{\beta,\gamma\text{-OHdPip}}$), two hydroxyl protons (OH-$3_{\beta,\gamma\text{-OHdPip}}$ and OH-$4_{\beta,\gamma\text{-OHdPip}}$), and a α-amino methine (H-$2_{\beta,\gamma\text{-OHdPip}}$) (Figure 1). This evidence in combination with key HMBC correlations from H-$3_{\beta,\gamma\text{-OHdPip}}$ to C-$1_{\beta,\gamma\text{-OHdPip}}$ (δ 166.6), C-$2_{\beta,\gamma\text{-OHdPip}}$ (δ 56.9), C-$4_{\beta,\gamma\text{-OHdPip}}$ (δ 62.6) and C-$5_{\beta,\gamma\text{-OHdPip}}$ (δ 147.2) revealed the presence of a rare 4,5-dihydroxy-2,3,4,5-tetrahydropyridazine-3-carboxylic acid (β,γ-OHdPip). While monohydroxylated δ,ε-dehydropiperazic acids have been reported in kutznerides,[4a] luzopeptides,[4b] and quinoxapeptides,[4c] to the best of our knowledge, this report represents the first occurrence of a β,γ-dihydroxydehydro piperazic acid.

Long-range correlations between α-protons to carbonyl carbons of adjacent amino acids led us to establish the following partial sequence for **1**: γ-ClPip-Ala-β,γ-OHdPip-Haa. Moreover, inter-residue ROE correlations of NH-$2_{\alpha\text{-MeSer}}$ (δ 7.68) to H-2_{Pip} (δ 4.90) and of NH-5_{Pip} (δ 4.67) to H-$2_{\gamma\text{-ClPip}}$ (δ 5.73), together with HMBC correlations from NH-$2_{\alpha\text{-MeSer}}$ to C-1_{Pip} (δ 168.9) and NH-5_{Pip} to C-$1_{\gamma\text{-ClPip}}$ (δ 171.8), linked the partial sequence α-MeSer-Pip to the C-terminus of γ-ClPip. Finally, the downfield chemical shifts of the oxygenated methylene protons at δ 5.30 and 4.64 along with a HMBC correlation from the later protons to δ 171.9 indicated an ester linkage between C-2_{Haa} and C-$1_{\alpha\text{-MeSer}}$. Upon these spectroscopy data, the structure of **1** was characterized as an 18-membered cyclic depsipeptide. With the amino acid sequence of **1** in hand, it was evident that svetamycin A was structurally related to the piperazimycins, which were isolated from a marine *Streptomyces*,[5] and to the gerumycins that were isolated from an ant-associated *Pseudonocardia*.[6]

Table 1. NMR spectroscopic data (500 MHz, DMSO-d_6) for Svetamycin A (1)

position	δ_C[a]	δ_H[b] (*J* in Hz)	HMBC[c]	ROESY[d]
	α-MeSer			
1	171.9			
2	60.4			
3a	63.6	3.67 dd (11.0, 7.5)	1, 2, 4	3b, 4, NH-2, OH-3
3b		3.82 dd (11.0, 5.7)	1, 2, 4	3a, 4, NH-2, OH-3
4	19.7	1.42 s	1, 2, 3	3ab, NH-2
NH-2		7.68 s	1, 2, 3, 4, 1_{Pip}	3ab, 4,OH-3, 2_{Pip}, $3b_{Pip}$
OH-3		4.57 t (6.5)	2, 3	3ab, 4, NH-2
	Pip			
1	168.9			
2	50.9	4.90 m	1, 3, 4	3a,3b, 4b, NH-5, NH-$2_{\alpha\text{-MeSer}}$
3a	24.4	1.72 m	1, 2, 4, 5	2, 3b, 4a, 5a
3b		2.19 m		2, 3a, 4a, NH-$2_{\alpha\text{-MeSer}}$
4a	20.2	1.35 m		3b, 4b, 5ab
4b		1.68 m	3, 5	2, 3b, 4a, 5b, NH-5
5a	46.3	2.61 m		3a, 4a, 5b, $2_{\gamma\text{-ClPip}}$
5b		2.94 br d (12.7)	3, 4	4ab, 3a, 5a, NH-5
NH-5		4.67[e]	$1_{\gamma\text{-ClPip}}$, $5_{\gamma\text{-ClPip}}$	3a, 5b, $2_{\gamma\text{-ClPip}}$
	γ-ClPip			
1	171.8			
2	49.8	5.73 dd (5.5, 1.2)	1, 3, 4, 1_{Ala}	3ab, NH-5_{Pip}
3a	34.5	1.90 td (11.8, 5.5)	1, 2, 4, 5	2, 3b, 5a

3b		2.41 ddd (11.8, 4.6, 1.2)	2, 4, 5	2, 3a, 4
4	52.5	4.36 tt (11.4, 4.6)	3, 5	3b, 5b, NH-5
5a	54.0	2.66 td (12.8, 11.6)	3, 4	3a, 5b, 3_{Ala}
5b		3.38 ddd (11.6, 4.7, 1.8)	3, 4	4, 5a, NH-5
NH-5		5.23 dd (12.8, 1.4)	5, 1_{Ala}	4, 5b
	Ala			
1	172.7			
2	43.1	5.33[e] dq (8.3, 6.9)	1, 3, $1_{\beta\gamma\text{-OHdPip}}$	3, NH-2, $2_{\beta\gamma\text{-OHdPip}}$
3	17.9	1.18 d (6.9)	1, 2	2, NH-2
NH-2		8.15 d (8.3)	1, 2, $1_{\beta\gamma\text{-OHdPip}}$	2, 3, $2_{\beta\gamma\text{-OHdPip}}$, $3_{\beta\gamma\text{-OHdPip}}$
	β,γ-OHdPip			
1	166.6			
2	56.9	4.71 br d (5.4)	1, 3, 4	3, 4, OH-3, NH-2_{Ala}
3	63.8	4.06 q (4.3)	1, 2, 4, 5	2, 4, 5, NH-2_{Ala}, OH-3, OH-4
4	62.6	3.93 m	2, 3, 5	2, 3, 5, OH-3, OH-4
5	147.2	6.97 d (2.3)	3, 4	3, 4, OH-4
OH-3		5.27 d (4.2)	1, 2, 3, 4	2, 3, 4
OH-4		5.80 d (8.6)	3, 4, 5	3, 4, 5
	Haa			
1	166.7			
2a	61.5	4.64 d (15.6)	1, $1_{\alpha\text{-MeSer}}$	2b, $5b_{Pip}$, $2_{\gamma\text{-ClPip}}$
2b		5.30 d (15.6)	1, $1_{\alpha\text{-MeSer}}$	2a

[a]Recorded at 175 MHz; referenced to residual DMSO-d6 at δ 39.51 ppm. [b]Recorded at 500 MHz; referenced to residual DMSO-d6 at δ 2.50 ppm. [c]Proton showing HMBC correlation to indicated carbon. [d]Proton showing ROESY correlation to indicated proton. [e]Signal overlapped

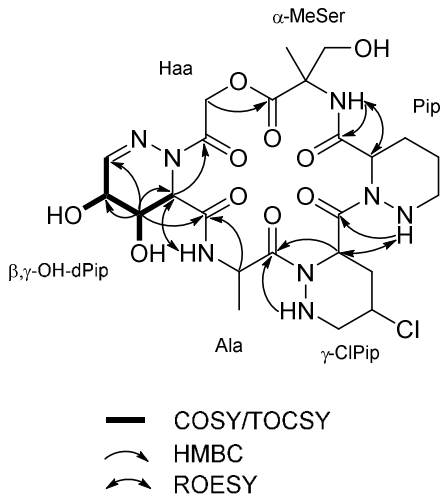

Figure 1. Key 2D NMR data to establish the structure of β,γ-OHdPip and the connectivity of the residues in **1**.

The configurations of the stereogenic centers of **1** were solved using a combination of methods. The absolute configurations of α-MeSer and Ala were deduced as L by LC-MS comparison of L- and D-FDLA (1-fluoro-2,4-dinitrophenyl-5-L/D-leucinamide) derivatives of the acid hydrolysate of **1** with authentic standards (Advanced Marfey's method).[7] The L- and D-FDLA derivatives of Pip were detected at retention times of 31.5 and 29.0 min on the reconstructed ion chromatogram for *m/z* 425 $[M + H]^+$, respectively (see Advanced Marfey's Analysis, Experimental Section). As reported by Cai *et al,*[8] the L-FDLA derivative of the D-Pip should elute before the L-Pip derivative. Thus, the absolute configuration of Pip was determined to be L. To establish the absolute stereochemistry of γ-ClPip, we first established its relative configuration by analyzing ROESY spectrum and $^3J_{H,H}$ coupling constants. The equatorial position of H-$2_{\gamma\text{-ClPip}}$ was assigned on the basis of its intermediate and small $^3J_{H,H}$ coupling constants of (5.5 and 1.2 Hz). In addition, key ROE correlations between H-$2_{\gamma\text{-ClPip}}$/H-$3a_{\gamma\text{-ClPip}}$, H-$2_{\gamma\text{-ClPip}}$/H-$3b_{\gamma\text{-ClPip}}$, H-$5a_{\gamma\text{-ClPip}}$/H-$3a_{\gamma\text{-ClPip}}$, and H-$4_{\gamma\text{-ClPip}}$/NH-$5_{\gamma\text{-ClPip}}$ indicating H-$4_{\gamma\text{-ClPip}}$ was axial

(see Figure 2a). We then synthesized an authentic sample of (3*R*,5*S*)-5-chloropiperazic acid by using a variation of two previously described routes (see Scheme 1),[9] and applied the advanced Marfey's method which pointed out the presence of (3*R*,5*S*)-5-chloropiperazic acid.

Scheme 1. Synthesis of (3*R*,5*S*)-5-chloropiperazic acid

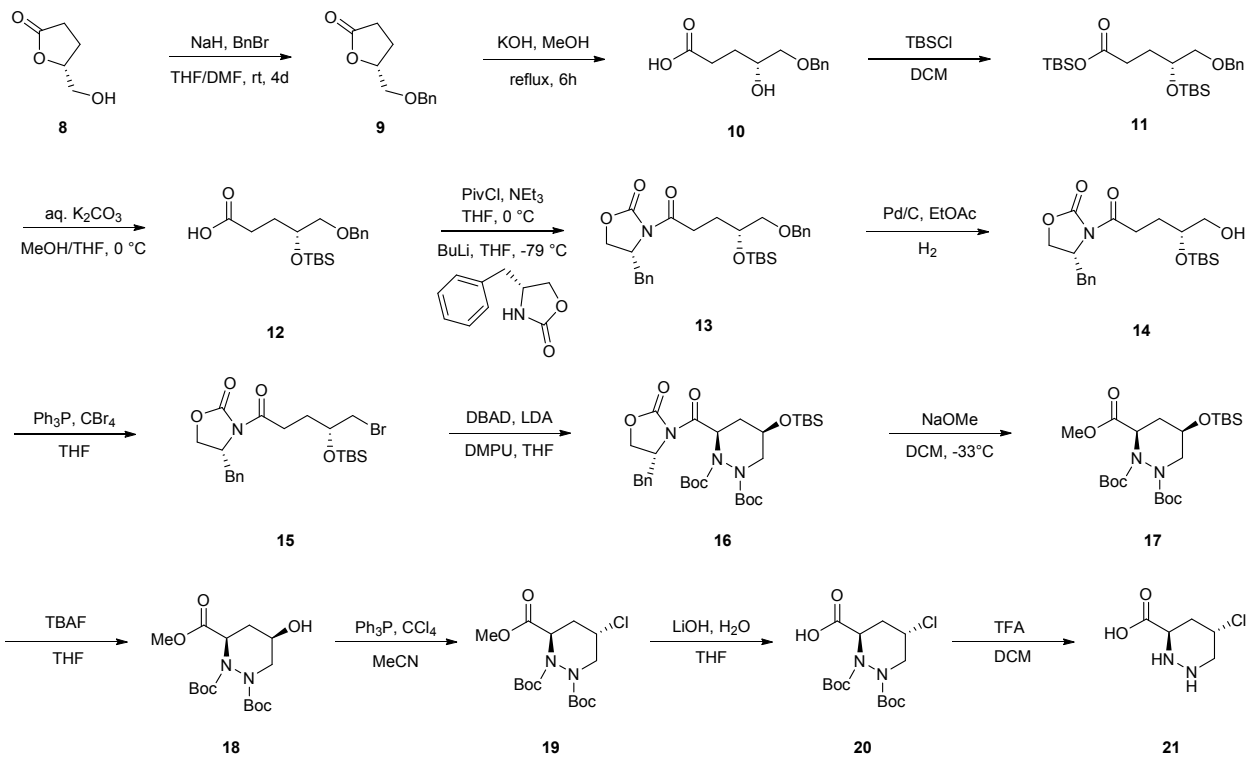

Once again ROE correlations and $^3J_{H,H}$ coupling constants were used to determine the relative configuration of β,γ-OHdPip. The intermediate $^3J_{H,H}$ coupling constant between H-2$_{\beta,\gamma\text{-OHdPip}}$ and H-3$_{\beta,\gamma\text{-OHdPip}}$ (5.5 Hz) along with strong ROE correlations between H-2$_{\beta,\gamma\text{-OHdPip}}$/H-4$_{\beta,\gamma\text{-OHdPip}}$ and H-3$_{\beta,\gamma\text{-OHdPip}}$/NH$_{Ala}$ indicated H-2$_{\beta,\gamma\text{-OHdPip}}$ and the hydroxyl group at C-3$_{\beta,\gamma\text{-OHdPip}}$ were pseudoaxial, whereas the hydroxyl group at C-4$_{\beta,\gamma\text{-OHdPip}}$ was pseudoequatorial (see Figure 2b).[10] Together, this NMR data indicated the relative configuration of the stereogenic centers in β,γ-OHdPip as 2*R**, 3*R**, 4*S**. Interestingly, this result highlighted a structural key difference of

svetamycins with respect to natural product cyclodepsipeptides, in which the α-proton of N^{α}-acyl-piperazic acid or N^{α}-acyl-δ,ε-dehydropiperazic acid is located in an equatorial or pseudoequatorial orientation due to a rotameric $A^{1,3}$-strain effect.[9b, 11] In particular, the piperazimycins and gerumycins, which have similar amino acid sequences and stereochemistry at comparable centers to svetamycin A, bear piperazate residues displaying axial orientations for the α-carboxamide groups.

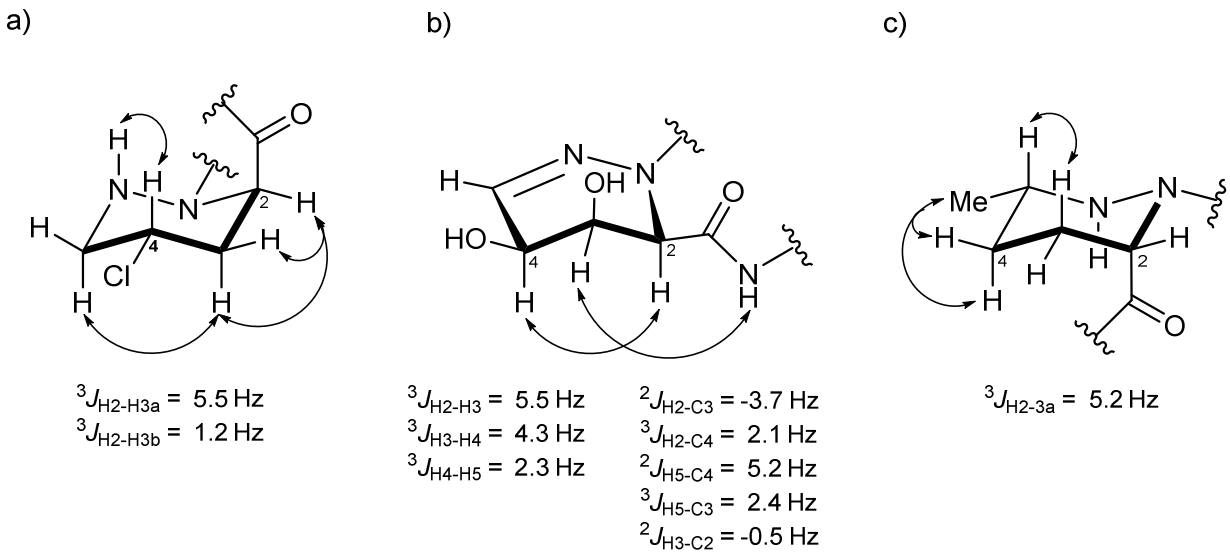

Figure 2. Key ROESY correlations and $^3J_{H-H}$ coupling constants to establish the relative stereochemistries of a) γ-ClPip, b) β,γ-OHdPip, and c) δ-MePip.

Furthermore, we employed a combined quantum-mechanical (QM)/NMR approach to compare experimental and calculated ^{13}C and ^1H NMR chemical shifts to corroborate the proposed configuration for the β,γ-OHdPip residue. Since the absolute configuration of α-MeSer, Pip, and γ-ClPip were already determined, the QM calculations were performed on eight possible diastereoisomers of **1** arising from the three stereocenters of β,γ-OHdPip (compounds **1a**-**1h**, see Figure S1). An extensive conformational search at the empirical level was carried out for **1a**-**1h**

by using Monte Carlo Molecular Mechanics (MCMM), Low-Mode Conformational Sampling (LMCS), and Molecular Dynamics (MD) simulations (see Computational Details, Experimental Section). All the obtained conformers were then submitted to a geometry and energy optimization step at the DFT (density functional theory) level. To obtain information on the stereochemistry of β,γ-OHdPip, ^{13}C and ^{1}H NMR chemical shifts were predicted at the M062X/6-31g(d,p) level for **1a-1h,** taking account the Boltzmann distribution of the conformers for each stereoisomer obtained at the same level of theory. Subsequently, the corrected mean absolute error (CMAE) values were used to compare calculated and experimental values (see Computational Details, Table 2 and Figure 3). As shown in Figure 3, isomer **1g** showed the lowest ^{13}C and ^{1}H CMAE values (1.60 ppm and 0.21 ppm, respectively), confirming the 2*R**, 3*R**, 4*S** as the most probable relative configuration at β,γ-OHdPip and suggesting 2*S*, 3*S*, 4*R* absolute configuration. To further corroborate our findings, we also employed the recently introduced DP4+ method that has proven to be a powerful tool for the correct stereochemical assignment of organic compounds.[14] Herein, we observed that isomer **1g** had the highest sDP4+ probabilities for both ^{13}C and ^{1}H (99.99% and 99.84%, respectively). These probabilities confirmed the absolute configuration of the residue β,γ-OHdPip as 2*S*, 3*S*, 4*R* with a high level of confidence.

In addition, a careful analysis of the energy- and geometry-optimized conformers **1a-1h** pointed out two main different arrangements of the β,γ-OHdPip residue for each of the conformers. In the first arrangement, named *Conf A*, the α-proton of β,γ-OHdPip is pseudoequatorial oriented, while in the second arrangement, termed *Conf B*, the proton H-$2_{\beta,\gamma\text{-OHdPip}}$ is pseudoaxial oriented (see Figure 4). Analysis of the conformers of **1g** on the basis of the experimental ROE data clearly indicated that only *Conf B* was in agreement with the ROE

correlation between H-$2_{\beta,\gamma\text{-OHdPip}}$/ H-$4_{\beta,\gamma\text{-OHdPip}}$. Besides, analysis of the energies of the conformers of **1g** at the M062X/6-31g(d,p) level of theory highlighted specific relative contributions of the *Conf A*/*Conf B* species on the final Boltzmann distribution (see Experimental section).[12,13] Interestingly, *Conf B* represented the main conformer in **1g** (relative weight on the final Boltzmann distribution: 69%), while *Conf A* which was not in agreement with the NMR data, represented the minor conformer (relative weight on the final Boltzmann distribution: 31%). Taken together, the reported data supports 2*S*, 3*S*, 4*R* as the most probable absolute configuration for β,γ-OHdPip residue.

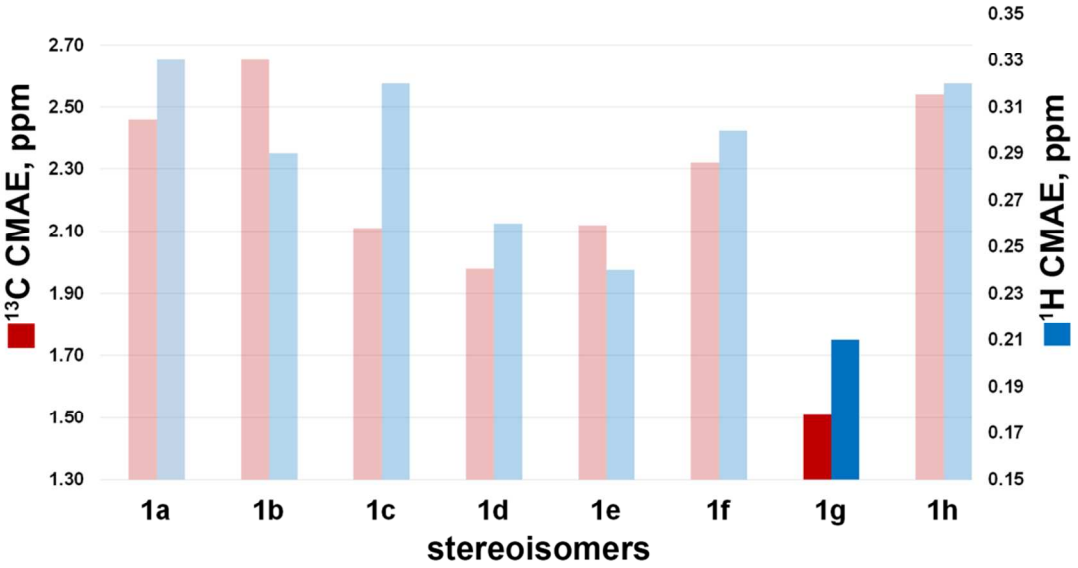

Figure 3. ^{13}C (opaque and transparent red bars) and ^{1}H (opaque and transparent blue bars) corrected mean absolute errors (CMAE) histograms related to compounds **1a-h**, as indicated in Table 2. CMAEs related to compound **1g** are highlighted with opaque colored bars.

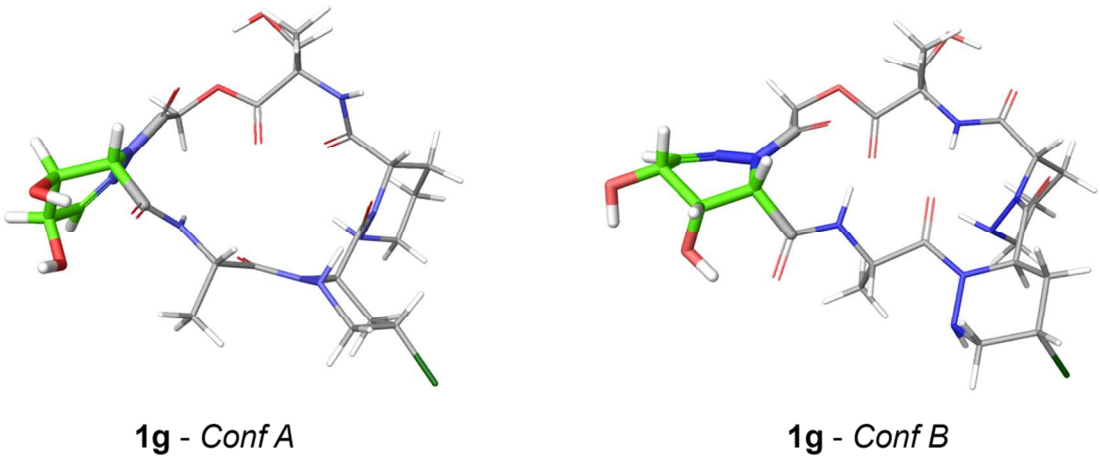

Figure 4. 3D representation of the most energetically favored conformers in **1g**.

Table 2. $^{13}C/^{1}H$ MAE (ppm) values, and DP4+ data reported for all the possible considered stereoisomers of compound 1 (1a-1h)

Stereoisomer	Configuration at β,γ-OHdPip	^{13}C CMAE (ppm)[a]	^{1}H CMAE (ppm)[b]	sDP4+ probability[c]		
				^{13}C data	^{1}H data	all data
1a	2*R*, 3*R*, 4*R*	2.46	0.33	0.00%	0.00%	0.00%
1b	2*R*, 3*R*, 4*S*	2.65	0.29	0.00%	0.00%	0.00%
1c	2*R*, 3*S*, 4*R*	2.11	0.32	0.00%	0.00%	0.00%
1d	2*R*, 3*S*, 4*S*	1.98	0.26	0.01%	0.00%	0.00%
1e	2*S*, 3*R*, 4*R*	2.12	0.24	0.00%	0.16%	0.00%
1f	2*S*, 3*R*, 4*S*	2.32	0.30	0.00%	0.00%	0.00%
1g	2*S*, 3*S*, 4*R*	1.51	0.21	99.99%	99.84%	100.00%
1h	2*S*, 3*S*, 4*S*	2.54	0.32	0.00%	0.00%	0.00%

[a] ^{13}C CMAE = $(\Sigma[|(\delta_{exp} - \delta_{scaled})|])/n$, summation of the absolute error values (difference of the absolute values between corresponding experimental, δ_{exp}, and scaled calculated, δ_{scaled}, ^{13}C chemical shifts), normalized to the number of considered chemical shifts (n); the related data are reported in Table S8. The δ_{scaled} values were obtained by the corresponding calculated chemical shift data (δ_{calcd}, see Computational Details); the latters were produced using the "multi standard" approach, using TMS as reference compound for sp^3 ^{13}C atoms, benzene for sp^2 ^{13}C atoms (excluding carbonyl carbons), and N-Methylformamide for carbonyl carbons. [b] ^{1}H CMAE = $\Sigma[|(\delta_{exp} - \delta_{scaled})|]/n$, summation of the absolute error values (difference of the absolute values between corresponding experimental, δ_{exp}, and scaled calculated, δ_{scaled}, ^{1}H chemical shifts), normalized to the number of considered chemical shifts (n); the related data are reported in Table S9 . The δ_{scaled} values were obtained by the corresponding calculated chemical shift data (δ_{calcd}, see Computational Details); the latters were produced using the "multi standard" approach, using

TMS as reference compound for sp^3 ^1H atoms, and benzene for ^1H atoms bound to sp^2 ^{13}C atoms. [c]sDP4+ probabilities related to the set of data reported in Table S8 (^{13}C chemical shift set of data) and Table S9 (^1H chemical shift set of data).

HR-ESI-MS and NMR data supported the molecular formula of $C_{25}H_{37}ClN_8O_{10}$ and $C_{26}H_{39}ClN_8O_{10}$ for compounds **2** and **3**, respectively. The NMR data clearly indicated that the amino acid sequences of **2** and **3** are the same as that of **1**, except for small changes in the resonances ascribable to the piperazic acid residue (see ^1H and ^{13}C NMR data at Table 3 and Table 5). Indeed, compound **2** contained an additional methyl group whereas **3** displayed two additional methyl groups, which explained the 14 and 28 amu mass differences with **1**. Furthermore, COSY and TOCSY correlations of **2** revealed a spin system starting from the aminomethine proton H-2 $_{\delta\text{-MePip}}$ (δ 4.88) to the secondary amine NH-5$_{\delta\text{-MePip}}$ (δ 4.88). Taken this data together with key HMBC correlations from the methyl protons at δ 1.00 (Me-5$_{\delta\text{-MePip}}$) to the methylene at 28.2 (C-4$_{\delta\text{-MePip}}$) and to the methine at 52.3 (C-5$_{\delta\text{-MePip}}$) established the presence of an unusual 6-methylhexahydropyridazine-3-carboxylic acid (δ-MePip). Therefore, svetamycin B (**2**) was assigned as a C-5$_{Pip}$ methyl analogue of **1**. In similar fashion, interpretation of the 2D NMR data of svetamycin C (**3**) allowed us to determine this compound as the C-5$_{Pip}$ dimethyl congener of **1**. To the best of our knowledge, this is the first report of either a δ-substituted piperazic acid or a methyl piperazic congener. Up to date, only γ-chloro and γ-hydroxy congeners of piperazic acid have been reported from peptide natural products.[15] The absolute configurations for L-α-MeSer, 3*R*,5*S*-γ-ClPip, and L-Ala in **2** and **3** were determined by using the advanced Marfey's method. The relative configuration of δ-MePip in **2** was determined by analysis of homonuclear coupling constants $^3J_{H,H}$ and ROE correlations. In particular, the

intermediate $^{3}J_{H,H}$ coupling constant of 5.2 Hz between H-2$_{\delta\text{-MePip}}$ and H-3a$_{\delta\text{-MePip}}$ together with ROE correlations between H-3a$_{\delta\text{-MePip}}$/H-5$_{\delta\text{-MePip}}$, H-4a$_{\delta\text{-MePip}}$/Me-5$_{\delta\text{-MePip}}$, and H-4b$_{\delta\text{-MePip}}$/Me-5$_{\delta\text{-MePip}}$ suggested an equatorial orientation for both H-2$_{\delta\text{-MePip}}$ and Me-5$_{\delta\text{-MePip}}$ (see Figure 2c). Also, the relative configurations of β,γ-OHdPip in **2** and **3** were deduced as 2*R**, 3*R**, 4*S** on the basis of ROE, correlations, $^{3}J_{H,H}$ coupling constants, and chemical shifts. Unfortunately, we were not able to establish the absolute configurations of neither δ-MePip in **2** nor δ,δ-dMePip in **3** by using Marfey's analysis.

Table 3. ^{1}H NMR Data (500 MHz, DMSO-d_6) for Svetamycins B-D (2-4)

position	2[a]	3[a]	4[a]
	δ_H (J in Hz)	δ_H (J in Hz)	δ_H (J in Hz)
	α-MeSer	α-MeSer	α-MeSer
1			
2			
3a	3.71 dd (10.7, 8.0)	3.61 dd (10.8, 6.4)	3.61 m
3b	3.81 dd (10.8, 5.6)	3.83 dd (10.8, 5.9)	3.88[b] m
4	1.43 s	1.37 s	1.46 s
NH-2	7.55 s	7.78 s	7.43 s
OH-3	4.44 br. dd (8.0, 5.5)	4.76[b] br. dd (6.2, 5.7)	4.06[b] m
	δ-MePip	δ,δ-dMePip	γ,ε-dPip
1			
2	4.88 br. dd (5.5, 1.4)	4.88 br. dd (5.4, 1.6)	4.99 br. dd (4.3, 1.1)
3a	1.76 m	1.96 m	1.82 m
3b	2.17 br. d (13.5)	2.07 dq (13.5, 2.2)	2.09[b] m
4a	1.36 m	1.34 dt (13.3, 3.2)	2.21 m
4b	1.51 br. dd (12.6,4.0)	1.42 br. dd (13.3, 4.0)	2.32 br. dd (11.6, 6.6)
5	2.69[b] m		7.12 br. d (2.8)
Me-5a	1.00[b] br. d (6.5)	1.00 br, s	
Me-5b		1.01 br. s	
NH-5	4.14 d (12.2)	4.57[b] s	
	γ-ClPip	γ-ClPip	γ-ClPip
1			
2	5.8 d (8.8)	5.83 br. s	5.77 br. s

3a	1.93 td (13.0, 6.0)	1.89 ddd (12.7, 11.2, 6.0)	2.10[b] m
3b	2.38 m	2.40 br. ddd (12.8, 4.5, 1.7)	2.50[b]
4	4.36 tt (11.2, 5.4)	4.46 tt (10.9, 4.6)	4.12 m
5a	2.67[b] m	2.69 td (12.7, 11.0)	2.72[b] m
5b	3.39 m	3.41 br. ddd (12.8, 4.4, 2.0)	3.35[b]
NH-5	5.27[b]	5.21[b]	5.48 br. dd (12.8, 1.4)
	Ala	Ala	Ala
1			
2	5.31 q (7.0)	5.38 q (7.0)	5.23 q (6.9)
3	1.19 br. d (6.9)	1.18 d (7.0)	1.19 br. d (6.9)
NH-2	7.94 br. d (6.9)	7.91 br. d (7.0)	8.06 br. d (6.9)
	β,γ-OHdPip	β,γ-OHdPip	β,γ-OHdPip
1			
2	4.67 d (4.8)	4.56[b] br. d (5.0)	4.88[b] br. s
3	4.05 q (4.3)	4.06 q (4.0)	4.02 m
4	3.94 m	3.95 m	3.91[b] m
5	6.97 br. d (2.0)	6.93 br. d (1.1)	7.05 br. d (2.8)
OH-3	5.27[b]	5.22[b]	5.41 br. s
OH-4	5.85 d (8.7)	5.73 d (8.3)	6.06 br. d (8.3)
	Haa	Haa	Haa
1			
2a	4.71 d (15.9)	4.73[b] d (16.2)	4.87[b] d (15.9)
2b	5.25[b] d (15.9)	5.18 d (16.2)	5.11 d (15.9)

[a]Recorded at 500 MHz; referenced to residual DMSO-d_6 at δ 2.50 ppm. [b]Signal overlapped

Table 4. ^{1}H NMR Data for Svetamycins E-G (5-7)

	5[a]	6[a]	7[b]
position	δ_H (J in Hz)	δ_H (J in Hz)	δ_H (J in Hz)
	α-MeSer	α-MeSer	α-MeSer
1			
2			
3a	3.53[c] d (10.8)	3.69 dd (11.0, 7.7)	4.06[c] s
3b	3.64 d (10.8)	3.78 dd (11.0, 5.8)	4.06[c]
4	1.35 s	1.43 s	1.54 s
NH-2	7.96 s	7.59 s	7.72 s
OH-1			
OH-3		4.55 br. dd (7.7, 5.8)	
	δ,δ-dMePip	Pip	δ,δ-dMePip
1			
2	4.88 br. s	4.92 m	5.04 br. dd (5.8, 1.6)
3a	2.00[c] m	1.72[c] m	1.99 m
3b	2.00[c] m	2.20 m	2.07 m
4a	1.38[c] m	1.35 m	1.46 m
4b	1.38[c] m	1.74[c] m	1.76 td (13.3, 3.5)
5a		2.61 m	
5b		2.95 m	
Me-5a	1.03 s		1.14 s
Me-5b	1.08 s		1.16 s
NH-5	4.64 s	4.60[c] br. dd (12.7, 1.6)	
	γ-ClPip	γ-BrPip	γ-BrPip
1			

2	5.80 br. dd (5.5, 2.3)	5.70 br. dd (6.2, 1.3)	5.86 br. dd (6.2, 1.5)
3a	1.97[c] m	2.05 td (12.8, 6.2)	2.20 ddd (13.5, 12.4, 6.2)
3b	2.65[c] m	2.50[c]	2.77 ddd (13.5, 4.0, 1.7)
4	4.24 tt (10.9, 4.5)	4.51 m	4.32 dddd (12.2, 10.5, 4.5, 4.1)
5a	2.68[c] m	2.82 q (12.3)	2.94 dd (13.4, 11.0)
5b	3.36[c]	3.45 m	3.45 br. dd (13.6, 4.4)
NH-5	5.49 br. dd (12.3, 1.8)	5.28[c] br. dd (12.3, 1.7)	
	Ala	Ala	Ala
1			
2	5.04 dq (8.5, 6.8)	5.35[c] dq (8.2, 6.9)	5.27 q (6.9)
3	1.16 d (6.8)	1.18 d (6.9)	1.33 d (6.9)
NH-2	7.59 d (8.5)	8.13 d (8.2)	
	β,γ-OHdPip	β,γ-OHdPip	β,γ-OHdPip
1			
2	4.75 br. d (5.2)	4.71 d (5.4)	4.99 br. d (5.7)
3	4.00 br. dd (5.2, 3.5)	4.05 q (4.6)	4.17 br. dd (5.7, 5.3)
4	3.96 t (3.3)	3.94 ddd (8.6, 4.5, 2.5)	4.02 br. dd (5.3, 3.0)
5	6.86 d (3.0)	6.97 d (2.5)	7.07 d (3.0)
OH-3		5.26[c] d (4.3)	
OH-4		5.81 d (8.6)	
	Haa	Haa	Haa
1			
2a	4.30 d (17.3)	4.61[c] d (15.8)	4.85[c] d (16.3)
2b	4.35 d (17.3)	5.37[c] d (15.8)	5.37 d (16.3)

[a]Recorded at 500 MHz; referenced to residual DMSO-d_6 at δ 2.50 ppm. [b]Recorded at 500 MHz; referenced to residual CD_3OD at δ 3.31 ppm. [c]Signal overlapped

Table 5. ^{13}C NMR Data for Svetamycins B-G (2-7).

	2[a]	3[a]	4[a]	5[a]	6[a]	7[b]
position	δ_C	δ_C	δ_C	δ_C	δ_C	δ_C
	α-MeSer	α-MeSer	α-MeSer	α-MeSer	α-MeSer	α-MeSer
1	172.0	171.9	172.2	173.5	171.8	172.4
2	60.5	59.8	60.6	60.1	60.5	61.5
3	63.9	63.4	63.8	64.6	64.3	63.0
4	19.1	19.9	19.0	19.6	19.3	17.4
	δ-MePip	δ,δ-dMePip	γ,ε-dPip	δ,δ-dMePip	Pip	δ,δ-dMePip
1	169.0	169.1	168.9	170.2	169.0	169.9
2	49.7	49.7	50.9	49.5	51.2	49.2
3	24.3	21.4	17.2	22.9	24.2	19.5
4	28.2	31.8	19.7	31.9	20.2	31.4
5	52.3	50.9	145.5	50.9	46.4	50.5
Me-5a		28.3		28.4		27.1
Me-5b	19.3	22.7		22.1		21.4
	γ-ClPip	γ-ClPip	γ-ClPip	γ-ClPip	γ-BrPip	γ-BrPip
1	171.4	171.7	170.6	172.0	171.3	173.8
2	49.7	48.8	50.2	49.1	51.0	50.3
3	34.7	34.2	34.4	34.8	35.6	35.1
4	52.6	52.3	52.5	52.5	45.2	41.9
5	54.1	54.0	53.4	53.6	54.7	53.9
	Ala	Ala	Ala	Ala	Ala	Ala
1	172.4	172.3	172.4	172.8	172.0	173.2
2	43.4	43.1	44.0	45.4	43.0	45.1

3	18.1	17.9	17.9	18.0	18.1	16.7
	β,γ-OHdPip	β,γ-OHdPip	β,γ-OHdPip	β,γ-OHdPip	β,γ-OHdPip	β,γ-OHdPip
1	166.3	166.4	166.9	165.3	166.3	166.6
2	56.9	56.9	55.9	55.1	56.7	55.8
3	63.7	63.7	63.0	65.2	63.8	62.9
4	62.4	63.0	61.3	62.3	62.6	60.9
5	146.9	147.1	146.4	144.2	146.8	145.3
	Haa	Haa	Haa	Haa	Haa	Haa
1	166.4	166.1	166.8	172.5	166.6	166.6
2	61.9	61.3	62.5	59.9	61.5	62.2

[a]Recorded at 175 MHz; referenced to residual DMSO-d_6 at δ 39.51 ppm. [b]Recorded at 175 MHz; referenced to residual CD_3OD at δ 49.15 ppm

Evident from the total ion chromatogram (TIC) obtained from the LC/MS, the methanol extract also contained two low abundance chlorinated compounds (**4**-**5**) eluting at considerably shorter retention times compared to **1**-**3**. The HR-ESI-MS spectrum of svetamycin D (**4**) suggested a molecular formula of $C_{24}H_{33}ClN_8O_{10}$ that differed from that of **1** by subtraction of two hydrogen atoms and required 12 degrees of unsaturation, one more than compound **1**. Although the 1D and 2D NMR spectra of **4** (see ^{1}H and ^{13}C NMR data at Table 3 and Table 5) contained small impurities, it clearly indicated that the amino acid sequence of **4** is the same as that of **1** except for the substitution in **4** of δ,ε-dehydropiperazic acid (δ,ε-dPip) for a piperazic acid residue in **1**. The HR-ESI-MS of compound **5** displayed a molecular ion at 677.2675 $[M+H]^+$ suggesting a molecular formula of $C_{26}H_{41}ClN_8O_{11}$. Examination of the NMR data of **5** (see ^{1}H and ^{13}C NMR data at Table 4 and Table 5) revealed that its amino acid sequence was

identical to that of **3**, although comparison of the ^{1}H and ^{13}C NMR chemical shifts of **3** and **5** showed differences in some resonances. In particular, the proton and carbon resonances corresponding to H-2_{Haac} in **5** (δ_H 4.33; δ_C 59.9) were shifted upfield in comparison to their respective ones in **3** (δ_H 4.73, 5.18; δ_C 61.3). Besides, the molecular formula of **5** required the presence of 10 degrees of unsaturation, one more than compound **3**. Taken together these data, svetamycin E (**5**) was determined as the acyclic analogue of svetamycin C (**3**). It is worth to mention that the respective acyclic congeners of **1** and **2** were detected by LC-HR-MS in a methanol extract of DSM14386. However, their low yields prevented their isolation and confirmation of their structure by NMR. An insufficient quantity of **5** prevented us from performing Marfey's analysis or to acquire ROESY data. Nevertheless, we assumed identical configurations for **3** and **5** at comparable stereogenic centers since their structures, and optical rotation values, and NMR data are quite similar.

LC-MS examination of the methanol extract from the bromide-enriched fermentation allowed us to identify two new brominated peptides. Svetamycin F (**6**) and svetamycin G (**7**) displayed in the ESI-MS spectrum an isotopic distribution of the ions $[M+H]^+$, 1:1, at *m/z* 675/677 and *m/z* 703/705, respectively, implying the presence of bromine. Their major ion peaks in the HR-ESI-MS spectrum were consistent with a molecular formula of $C_{24}H_{35}BrN_8O_{10}$ for **6** and $C_{26}H_{39}BrN_8O_{10}$ for **7**, which in turn differed from the molecular formula of **1** and **3**, respectively, by the replacement of chlorine with a bromine atom. Successively, comparison of the 2D NMR data (acquired in CD_3OD) of **6** to that of **1** determined that the bromine atom was located at the C-$4_{\gamma\text{-BrPip}}$ position (see ^{1}H and ^{13}C NMR data at Table 4 and Table 5). Indeed, the chemical shift for C-$4_{\gamma\text{-BrPip}}$ in **6** was ca 10 ppm upfield when compared to that of C-$4_{\gamma\text{-ClPip}}$ in **1**.[16] In similar fashion, 2D NMR data for **7** clearly determined svetamycin G to be the C-$4_{\gamma\text{-BrPip}}$-bromo-

derivative of **3**. We were unable to carry out Marfey's analysis on **6** and **7** due to the scarce amount of isolated material. However, we propose similar configurations for **6**, **7**, and **1** at comparable stereogenic centers on the basis of their NMR data (chemical shifts, ROE correlations, and $^3J_{H,H}$) and optical rotation values.

The biosynthetic origin of the piperazic acid units in the svetamycins was studied by feeding experiments with labeled precursors. LC-HR-ESI-MS/MS analysis of an extract prepared from a culture of *Streptomyces* sp. DSM14386 fed with L-[3,3,4,4,5,5-$^2H_6$]-ornithine revealed mass shifts for **1**-**3** indicating incorporation of ornithine. Exact determination of the mass shifts was complicated by the presence of three piperazic acid moieties and the chlorine isotopic pattern (see Figure S2). However, these results are consistent with the recently report by Walsh *et al.* that determined ornithine, and not glutamine, as the starting point in the biosynthesis of piperazic acid in *Kutzneria* spp. Indeed, it was demonstrated that formation of N^5-OH-Orn by the ornithine N-hydroxylase Ktzl, is the initial step for conversion of ornithine to piperazic acid.[17] Additionally, LC-HR-ESI-MS/MS analysis of compounds **1**-**3** obtained from an L-[methyl-$^2H_3$]-methionine feeding experiment showed mass shifts of 3 Da for **2** and of 6 Da for **3**, whereas for compound **1** no mass shift was observed (see Figure S3). These results prove that the introduction of the methyl groups in the piperazic acid units in the svetamycins is *S*-adenosyl-L-methionine (SAM)-dependent.

Microbroth dilution and microbial cell viability assays were used to evaluate the antimicrobial activity of compounds **1**, **3**, and **5**-**7** towards *M. smegmatis*, *E. coli*, *C. albicans*, and MRSA. The results are summarized in Table 6 and furnished insights in the structure-activity relationships of this structural class of piperazic acid-containing peptides. Svetamycin G (**7**) showed the most potent activity against *M. smegmatis* (IC_{80} = 2 μg/mL) whereas svetamycin C (**3**) and **7** were the

most potent antibiotics towards MRSA (MICs = 16 μg/mL). Svetamycin E (**5**) inhibited the growth of neither *M. smegmatis* nor MRSA at concentrations as high as 64 μg/mL, indicating that macrocyclization is needed for the antibiotic activity. Among the cyclic peptides, compound **7** was 4-16 times more potent than svetamycin F (**6**) while compound **3** was 4-fold more potent than svetamycin A (**1**). All together, these results revealed that methyl substitution of the piperazic acid unit at δ-position increases the activity. Finally, the weaker potency of **3** compared to **7** showed that replacement of chlorine by bromine has beneficial effects on the antimicrobial activity. Svetamycins A and C did not inhibit the growth of either *E. coli* or *C. albicans* at concentrations up to 64 μg/mL. Instead, the activity of the extract towards this Gram-negative pathogen was traced to the known pentalenolactone AA-57.[3]

Table 6. Antimicrobial activities for compounds 1, 3, and 5-7 (μg/mL)

	M. smegmatis (IC_{80})	MRSA (MIC)	*E. coli* (MIC)	*C. albicans* (MIC)	*M. tuberculosis* (IC_{80})
1	32	64	> 64	> 64	65.6
3	8	16	> 64	> 64	54.0
5	> 64	> 64	nd	nd	nd
6	32	64	nd	nd	nd
7	2	16	nd	nd	nd

nd = not determined

Although piperazic acid-containing cyclic peptides such as hytramycins and lydiamycins have been reported to exhibit anti-*Mycobacterium tuberculosis* activity,[8, 18] svetamycins A (**1**) and C (**3**) did show a very weak activity against the standard *M. tuberculosis* strain H37Rv with IC_{80}

values of 65 and 54 μg/mL, respectively (see Table 6). Also, compounds **1** and **3** were cytotoxic to a hepatoma cell line (HepG2) with IC_{50} values of 11.04 ± 4.02 and 3.59 ± 1.19 μg/mL.

CONCLUSION

In summary, we have discovered seven new halogenated piperazic acid-containing peptides, svetamycins A-G, that add to a small class represented by the piperazimycins and gerumycins. Svetamycins contain one hydroxyacetic acid residue, one alanine, and three tailored piperazate moieties, among which are the previously undescribed 6-methyl- and 6,6-dimethylhexahydropyridazine-3-carboxylic acids along with the unusual 4,5-dihydroxy-2,3,4,5-tetrahydropyridazine-3-carboxylic acid. The latter, is the first example of a piperazyl scaffold that in a peptide displays a pseudoequatorial conformation for the α-carboxamide group. In closing, this study also showed the utility of using a combined QM/NMR approach together with the DP4+ probability method for solving the configuration of stereogenic centers in natural products.

EXPERIMENTAL SECTION

General Experimental Procedures.

Optical rotations were measured with a Kruess LC-Serie 1 polarimeter, and IR spectra were obtained using a Fourier Transform (FT) Infrared Spectrometer (Japan Bunkou Ltd., JASCO FT/IR-420, ν_{max} 600-4.000 cm^{-1}, 20 °C) equipped with a Diamond ATR accessory. NMR spectra were recorded in DMSO-d_6 and CD_3OD on a Bruker Avance 500 MHz spectrometer equipped

with a 5 mm TXI cryoprobe. CQF- COSY, 2D-HOHAHA, HSQC, HMBC, and ROESY experiments were recorded using standard pulse programs. HSQC experiments were optimized for $^{1}J_{C\text{-}H}$ = 145 Hz, and HMBC spectra were optimized for $^{2,3}J_{C\text{-}H}$ = 8 and 6 Hz. UPLC-HR-MS data were obtained on a quadrupole time of flight spectrometer (LC-QTOF maXis II, Bruker Daltronics, Bremen, Germany) or a micrOTOF-LC spectrometer (Bruker Daltronics, Bremen, Germany) using a BEH C18 (150 x 2.1 mm, 1.7 µm column, Waters, Germany) with a linear gradient of 5-95% ACN + 0.1% FA at 450 μL/min in 18 min with UV detection in 205-640 nm range. Mass spectra were acquired using the ESI source in the range from 50–2000 *m/z*. HPLC for separation and purification was performed on a semi-preparative Agilent 1200 HPLC system equipped with a Jupiter Proteo C12 column (250 x 25 mm, 4 μm, DAD at 220 and 254 nm). All solvents used for separation and purification were analytical grade. The Marfey's analysis was performed in positive mode on an Agilent Series LC/MSD VL mass spectrometer (Agilent Technologies, Santa Clara, California).

Bacterial Strains and Cell Line. *Streptomyces* sp. DSM14386 was bought from the Leibniz Institute DSMZ-German Collection of Microorganisms and Cell Cultures, Braunschweig, Germany. *Staphylococcus aureus* ATCC 33582, *Escherichia coli* ATCC 53218, *Mycobacterium smegmatis* ATCC 607 and *Mycobacterium tuberculosis* H37Rv ATCC 27294 and the human liver cancer cell line HepG2 ATCC HB8065 were bought from the American Type Culture Collection, Manassas, Virginia. *Candida albicans* FH 2173 is from the strain collection of Sanofi-Aventis Deutschland GmbH, Industriepark Höchst, Germany.

Cultivation and Extraction. Pre-cultures of *Streptomyces* sp. DSM14386 were conducted in 0.3 L Erlenmeyer flasks with 0.1 L of pre-culture medium (20 g/L glucose, 5 g/L meat extract, 5 g/L yeast extract, 5 g/L peptone, 3 g/L caseine, 1.5 g/L NaCl, at pH 7.5) followed by incubation

for 4-7 days on a rotary shaker at 180 rpm and 28°C. The inoculation of the main fermentation with the pre-cultures was conducted in forty 2 L Erlenmeyer flasks, containing 0.5 L of the main-culture medium (30 g/L glycerol, 5 g/L $CaCO_3$, 15 g/L soybean meal, 2 g/L NaCl, at pH 7.5) followed by incubation on the rotary shaker at 180 rpm and 28°C for 7 days. After 7 days' fermentation, the cells and the supernatant were separated by centrifugation, followed by addition of a mixture of 2 % Amberlite® XAD 16 and XAD 7 (1:1) to the supernatant and stirring overnight. The resin was harvested afterwards, washed with H_2O, lyophilized, extracted with MeOH and dried under reduced pressure to yield 4 g.

Cultivation on Agar plates and Extraction. Main-culture medium supplemented with 1.5% of agar was used to conduct static fermentations in twenty agar plates (24 x 24 cm, Nunc). After the incubation at 28°C for 7 days, the agar cultures were harvested and extracted by adding 4 L H_2O and homogenizing by vigorous stirring. Once homogenized, extraction was performed by the addition of 4 L EtOAc and stirring overnight, followed by centrifugation and evaporation of the EtOAc to yield 18 g of dry extract.

Cultivation on NaBr Agar plates and Extraction. An additional static fermentations was conducted on ten agar plates (24 x 24 cm, Nunc) replacing 1.5 g/L NaCl with 1.5 g/L NaBr. After the incubation at 28°C for 7 days, the agar cultures were harvested and extracted by adding 2.0 L H_2O and homogenizing by vigorous stirring. Once homogenized, extraction was performed by the addition of 2.0 L EtOAc and stirring overnight, followed by centrifugation and evaporation of the EtOAc to yield 6.1 g of dry extract.

Isolation. The extracts prepared from liquid and solid fermentations were fractionated over a Sephadex LH-20 column (150 x 10 cm), respectively, using MeOH as eluting solvent. Fractions

containing the peptides were purified by semi-preparative reversed-phase HPLC (Jupiter Proteo C12, 250 x 25 mm, 4 μm, DAD at 220 and 254 nm) eluting with a linear gradient of 50-85% MeOH/H_2O with 0.05% TFA in 35 min to yield compounds **1** (3.69 mg, t_R = 17.3 min), **2** (0.42 mg, t_R = 22.4 min), **3** (0.93 mg, t_R = 24.9 min), **4** (0.25 mg, t_R = 13.2 min), **5** (0.40 mg, t_R = 15.3 min), **6** (0.81 mg, t_R = 19.5 min) and **7** (0.26 mg, t_R = 26.2 min).

*Svetamycin A (**1**)*. colorless, amorphous powder; $[\alpha]^{23}_D$ -3.3 (*c* 0.009, MeOH); LC-UV [(MeOH in H_2O+0.05% TFA)] λ_{max} 213, 240 nm; IR (film) ν_{max} 3265, 2949, 2359, 2341, 1734, 1672, 1630, 1558, 1419, 1247, 1202, 1126, 1018, 913 cm^{-1}; ^1H and ^{13}C NMR data, see Table 1; HRMS (ESI-TOF) *m/z*: $[M+Na]^+$ calcd for $C_{24}H_{35}ClN_8O_{10}Na$ 653.2057; found 653.2059.

*Svetamycin B (**2**)*. colorless, amorphous powder; $[\alpha]^{23}_D$ -5.2 (*c* 0.002, MeOH); LC-UV [(MeOH in H_2O+0.05% TFA)] λ_{max} 213, 240 nm; IR (film) ν_{max} 3264, 2948, 2360, 2341, 1739, 1689, 1641, 1540, 1436, 1205, 1135, 842 cm^{-1}; ^1H NMR data, see Table S2; HRMS (ESI-TOF) *m/z*: $[M+Na]^+$ calcd for $C_{25}H_{37}ClN_8O_{10}Na$ 667.2213; found 667.2225.

*Svetamycin C (**3**)*. colorless, amorphous powder; $[\alpha]^{23}_D$ -2.4 (*c* 0.004, MeOH); LC-UV [(MeOH in H_2O+0.05% TFA)] λ_{max} 213, 240 nm; IR (film) ν_{max} 3269, 2967, 2359, 2341, 1745, 1673, 1633, 1541, 1417, 1244, 1200, 1128, 1055, 939 cm^{-1}; ^1H NMR data, see Table S3; HRMS (ESI-TOF) *m/z*: $[M+Na]^+$ calcd for $C_{26}H_{39}ClN_8O_{10}Na$ 681.2369; found 681.2374).

*Svetamycin D (**4**)*. colorless, amorphous powder; $[\alpha]^{23}_D$ -8.8 (*c* 0.001, MeOH); LC-UV [(MeOH in H_2O+0.05% TFA)] λ_{max} 213, 240 nm; IR (film) ν_{max} 3360, 2937, 2360, 2341, 1678, 1635, 1558, 1421, 1244, 1200, 1126, 1058, 963 cm^{-1}; ^1H and ^{13}C NMR data, see Table 3 and Table 5; HRMS (ESI-TOF) *m/z*: $[M+Na]^+$ calcd for $C_{24}H_{33}ClN_8O_{10}Na$ 651.1900; found 651.1864.

*Svetamycin E (**5**)*. colorless, amorphous powder; $[\alpha]^{23}_{D}$ -5.5 (*c* 0.002, MeOH); LC-UV [(MeOH in H_2O+0.05% TFA)] λ_{max} 213, 240 nm; IR (film) ν_{max} 3387, 2945, 2360, 2341, 1647, 1523, 1407, 1290, 1200, 1137, 1013, 950 cm^{-1}; ^1H NMR data, see Table S4; HRMS (ESI-TOF) *m/z*: $[M+Na]^+$ calcd for $C_{26}H_{41}ClN_8O_{11}Na$ 699.2476; found 699.2497.

*Svetamycin F (**6**)*. colorless, amorphous powder; $[\alpha]^{23}_{D}$ -10.8 (*c* 0.004, MeOH); LC-UV [(MeOH in H_2O+0.05% TFA)] λ_{max} 213, 240 nm; IR (film) ν_{max} 3268, 2970, 2359, 2341, 1747, 1673, 1643, 1541, 1417, 1245, 1201, 1128, 1055, 1014, 944 cm^{-1}; ^1H NMR data, see Table S5 and S6; HRMS (ESI-TOF) *m/z*: $[M+Na]^+$ calcd for $C_{24}H_{35}BrN_8O_{10}Na$ 697.1552; found 697.1530.

*Svetamycin G (**7**)*. colorless, amorphous powder; $[\alpha]^{23}_{D}$ -16.9 (*c* 0.001, MeOH); LC-UV [(MeOH in H_2O+0.05% TFA)] λ_{max} 213, 240 nm; IR (film) ν_{max} 3328, 2963, 2358, 2341, 1748, 1666, 1627, 1540, 1437, 1412, 1246, 1201, 1127, 1013, 928 cm^{-1}; ^1H NMR data, see Table S7; HRMS (ESI-TOF) *m/z*: $[M+Na]^+$ calcd for $C_{26}H_{39}BrN_8O_{10}Na$ 725.1865; found 725.1884.

Synthesis of (3*R*,5*S*)-5-chloropiperazic acid (21). (3*R*,5*S*)-5-chloropiperazic acid was synthesized by using a variation of two previously described routes.[9] In brief, NaH (ca. 60% dispersion in mineral oil, 1.38 g, ca. 34.5 mmol) was added to a solution of (*R*)-dihydro-5-(hydroxymethyl)-furanone (**8**) (2 g, 17.2 mmol) in 14 mL of DMF and 10 mL of THF under Ar. Subsequently, benzyl bromide (4.1 mL, 34.5 mmol) and TBAI (0.64 g, 1.7 mmol) were added and the mixture was stirred for 4 days at rt. The reaction was then quenched with a phosphate buffer solution (pH 7, 10 mL), diluted with DCM (4 x 50 mL), and washed with water (3 x 15 mL). The organic phase was dried over Na_2SO_4 and concentrated under reduced pressure. The organic residue was then purified by SiO_2 flash chromatography using gradient elution with 10:1,

5:1, 1:1 petrol:EtOAc to afford 1.75 g (49 %) of the protected lactone **9** as a yellowish oil. Conversion of **9** into **13** was carried out following the synthetic route reported by Andreou *et al*.[9a] Hydrogenation of **13** (1.8 g, 3.62 mmol) in EtOAc (36 mL) was performed in an H_2-reactor with Pd/C (0.019 g, 0.18 mmol). The mixture was vigorously stirred at 4 bar overnight. The mixture was then filtered through celite and concentrated under reduced pressure. The residue was purified by SiO_2 flash chromatography using gradient elution with 8:1, 5:2, 1:1 petrol/EtOAc to afford 0.94 g (63.7 %) of the primary alcohol **14** as a yellowish oil. Subsequent conversion of **14** into **19** was performed as reported by Hale *et al*.[9b] To obtain **20**, LiOH.H_2O (0.03 g, 0.06 mmol) was added to a stirred solution of **19** (0.08 g, 0.02 mmol) in THF (1.40 mL) and H_2O (0.70 mL) at 0 °C, and stirred for 75 min. The reaction mixture was then acidified to pH 2 with a 10% aqueous HCl and in turn extracted with EtOAc (3 x 30 mL) and CH_2CL_2 (30 mL). The combined organic layers were dried with Na_2SO_4, filtered, concentrated under reduced pressure, and purified by RP-HPLC (Synergy Fusion C18, 250 x 25 mm, 4 μm, DAD at 220 and 254 nm, eluting with a linear gradient of 50-85% MeCN/H_2O with 0.05% TFA in 25 min and then isocratic) to yield compound **20** (0.03 g, t_R = 26.2 min).

*Compound **20**.* $[\alpha]^{25}_D$ +7.17°(*c* 0.151, CH_2Cl_2) ^{1}H NMR (500MHz, DMSO-d_6) δ = 4.63 (1H, br. t, J = 3.6 Hz, H_3), 4.12 (1H, dd, J = 10.2, 3.8 Hz, H_5), 3.38 (1H, dd, J = 14.2, 2.8 Hz, H_{6eq}), 3.16 (1H, br. dd, J = 14.2, 4.0 Hz, H_{6ax} overlapped), 2.30 (1H, ddd, J = 14.5, 10.5, 3.6 Hz, H_{4eq}), 2.23 (1H, dt, J = 14.5, 4.5 Hz, H_{4ax}), 1.43, 1.46 and 1.37 (18H, 2 x s, -OC(<u>Me</u>)$_3$ overlapped)

TFA (0.12 mL, 1.5 mmol) was added to a stirred solution of **20** (0.03 g, 0.007 mmol) in DCM at rt and under Ar , stirring for 1 h. Evaporation *in vacuo* afford 0.03 g of the (3*R*,5*S*)-5-chloro-piperazic acid trifluoroacetic acid salt **21**.

*Compound **21***. ^{1}H NMR (500MHz, CD_3OD) δ = 4.54 (1H, q, J = 7.5, 4.0 Hz, H_5), 4.27 (1H, dd, J = 9.2, 5.0 Hz, H_3), 3.48 (1H, dd, J = 14.5, 2.8 Hz, H_{6eq}), 3.27 (1H, br. dd, J = 14.5, 4.0 Hz, H_{6ax}), 2.46 – 2.41 (2H, m, H_{4eq} and H_{4ax})

Feeding experiments. A solution of 33 μl L-[methyl-$^2H_3$]methionine (0.03 mol/L, 45.7 mg, 400 μL DMSO/H_2O 1:3) was added on day 0, 2 and 4 to a 10 mL DSM14386 culture and cultivated for 7 days in total at 28°C and 180 rpm. After 7 days the culture broth was lyophilized and extracted with MeOH to generate dry extract. The extract was analyzed using UHR-ESI-MS.

A solution of 33 μl L-[3,3,4,4,5,5-$^2H_6$]-ornithine (0.03 mol/L, 52.4 mg, 400 μL DMSO/H_2O 1:3) was added on day 0, 2 and 4 to a 10 mL DSM14386 culture and cultivated for 7 days in total at 28°C and 180 rpm. After 7 days the culture broth was lyophilized and extracted with MeOH to generate dry extract. The extract was analyzed using UHR-ESI-MS.

Advanced Marfey's Analysis. Approximately 0.3 mg of **1** was dissolved in 200 μl MeOH, transferred to a 10 mL round flask, dried and hydrolyzed with 800 μL HCl (6 N). The round flask was placed for 16 hours in a preheated oven at 110 °C. After the hydrolysis, the solution was transferred to a glass vial, dried and dissolved in 100 μL H_2O and divided into two portions. To 50 μL of hydrolyzed **1** 20 μL $NaHCO_3$ (1 N) and 100 μL of a 1% 1-fluoro-2,4-dinitrophenyl-5-L-leucinamide (L-FDLA or D-FDLA solution in acetone) was added to each portion. The thus prepared samples were derivatized in the dark at 40°C for 40 min, cooled to room temperature, neutralized with 20 μL HCl (2 N) and dried in vacuum. Residues were dissolved in 50 μL MeOH. Analyses of the L- and L/D-FDLA (mixture of L- and D-FDLA) derivatives were performed using a Phenomenex Jupiter Proteo C12 column (4 μm, 250 x 4.6 mm,) with a linear gradient of 25-70% ACN/H_2O with 0.05% TFA in 35 min at a flow rate of 0.5 mL/min. An Agilent Series LC/MSD VL mass spectrometer was used for detection in positive mode.

Retention times (t_R, min) of the FDLA-derivatized amino acids for svetamycin A-C (1-3): L-Alanine 31.9, D-Alanine 35.8 *m/z* 384 $[M+H]^+$, L-*N*-Methyl-L-serin 27.2, D-*N*-Methyl-L-serin 29.6 *m/z* 414 $[M+H]^+$, L-(3*R*,5*S*)-Cl-piperazic acid 30.9, D-(3*R*,5*S*)-Cl-piperazic acid 33.9 *m/z* 459 $[M+H]^+$. Retention time (t_R, min) of the FDLA-derivatized piperazic acid for svetamycin A (1): L-piperazic acid 31.5, D-piperazic acid 29.0 *m/z* 425 $[M+H]^+$.

Computational Details. Maestro 10.2[19] was used for generating the starting 3D chemical structures of all possible relative diastereoisomers of compounds **1**. In particular, we considered the eight diastereoisomers arising from the combination of the three stereocenters on the β,γ-OHdPip moiety, named: **1a** (2*R*, 3*R*, 4*R*- β,γ-OHdPip), **1b** (2*R*, 3*R*, 4*S*- β,γ-OHdPip), **1c** (2*R*, 3*S*, 4*R*- β,γ-OHdPip), **1d** (2*R*, 3*S*, 4*S*- β,γ-OHdPip), **1e** (2*S*, 3*R*, 4*R*- β,γ-OHdPip), **1f** (2*S*, 3*R*, 4*S*- β,γ-OHdPip), **1g** (2*S*, 3*S*, 4*R*- β,γ-OHdPip), **1h** (2*S*, 3*S*, 4*S*- β,γ-OHdPip) (Figure S1, Supporting Information). Optimization of the 3D structures was performed with MacroModel 10.2[20] using the OPLS force field and the Polak-Ribier conjugate gradient algorithm (PRCG, maximum derivative less than 0.001 kcal/mol). Starting from the obtained 3D structures, we performed conformational searches at the empirical molecular mechanics (MM) level with Monte Carlo Multiple Minimum (MCMM) method (50000 steps) and Low mode Conformational Search (LMCS) method (50000 steps), allowing a full exploration of the conformational space. Moreover, molecular dynamics simulations were performed at 450, 600, 700, 750 K, with a time step of 2.0 fs, an equilibration time of 0.1 ns, and a simulation time of 10 ns. A constant dielectric term of DMSO, mimicking the presence of the solvent, was used in the calculations to reduce artifacts. For each diastereoisomer, all the conformers obtained from the above mentioned conformational searches were minimized (PRCG, maximum derivative less than 0.001 kcal/mol) and compared. We used the "Redundant Conformer Elimination" module of MacroModel 10.2[20]

to select non-redundant conformers, specifically excluding those differing more than 21.0 kJ/mol (5.02 kcal/mol) from the most energetically favoured conformation and setting a 0.5 Å RMSD (root-mean-square deviation) minimum cut-off for saving structures. The following mentioned QM calculations were performed using Gaussian 09 software.[21] Firstly, the selected conformers from MM experiments were optimized at QM level using the MPW1PW91 functional and the 6-31G(d) basis set.[22] Experimental solvent effects (DMSO) were reproduced using the integral equation formalism version of the polarizable continuum model (IEFPCM)[23]. After this step at the QM level, the obtained optimized geometries were visually inspected to remove further possible redundant conformers. All the selected conformers from the optimization step for the different diastereoisomers of compounds **1a-1h** were accounted for the subsequent computation of the ^{13}C and ^{1}H NMR chemical shifts, using the M062X functional and the 6-31G(d,p) basis set. Final ^{13}C and ^{1}H NMR spectra for each of the investigated diastereoisomers were built considering the influence of each conformer on the total Boltzmann distribution taking into account the relative energies (M062X/6-31G(d,p)). Calibrations of calculated ^{13}C and ^{1}H chemical shifts were performed following the multi-standard approach (MSTD).[24] In particular, sp^2 ^{13}C (excluding carbonyl carbons) chemical shift data were computed using benzene as reference compound,[24, 25] carbonyl ^{13}C chemical shift data using N-Methylformamide as reference, and the remaining ^{13}C chemical shift data using tetramethylsilane (TMS) as reference. On the other hand, ^{1}H chemical shifts related to hydrogens bound to sp^2 ^{13}C were computed using benzene as reference compound, while TMS was used for the remaining ^{1}H chemical shift data. Subsequently, the scaled ^{13}C and ^{1}H NMR chemical shifts (δ_{scaled}) were obtained by a linear fit of the calculated (δ_{calcd}) versus experimental (δ_{exp}) ^{13}C NMR chemical shifts. The intercept (b) and slope (a) were determined and used to state the empirically scaled theoretical chemical

shifts: $\delta_{scaled} = (\delta_{calcd} - b)/a$. Experimental and calculated ^{13}C and ^{1}H NMR chemical shifts were then compared computing the $\Delta\delta$ parameter (see Tables S8-S9, Supporting Information): $\Delta\delta = |\delta_{exp} - \delta_{scaled}|$ where, δ_{exp} (ppm) and δ_{scaled} (ppm) are the $^{13}C/^{1}H$ experimental and scaled calculated chemical shifts, respectively. The corrected mean absolute errors (CMAEs) for all the possible diastereoisomers (see Table 2) were computed:

$$\mathrm{CMAE} = \frac{\sum(\Delta\delta)}{\mathrm{n}}$$

defined as the summation through n of the absolute error values (difference of the absolute values between corresponding experimental and scaled calculated ^{13}C-^{1}H chemical shifts), normalized to the number of the chemical shifts considered (n). Furthermore, sDP4+ (DP4+ related to scaled shifts) probabilities related to all the stereoisomers of **1** were computed considering both ^{13}C and ^{1}H chemical shifts, and comparing them with the related experimental data (Table 2)

Antimicrobial Assays. Stock solutions of the compounds were prepared at 6.4 mg/mL in DMSO (Sigma-Aldrich, Germany) and used to perform the biological testing in duplicates (64 - 0.03 μg/mL) in 100 μL cation-adjusted Müller-Hinton broth (Becton, Dickinson and Company, Germany) containing a suspension of *S. aureus* ATCC 33582 (~5 × 105 cells/mL), *E. coli* ATCC53218 (~5 × 10^5 cells/mL) or *C. albicans* FH 2173 (~1 × 106 cells/mL) on 96-well round bottom plates. The plates were incubated with shaking (180 rpm) at 37°C for 18 h, and the minimum inhibitory concentrations (MICs), defined as the lowest concentration inhibiting the visible growth the microorganisms, determined. For testing against *M. smegmatis*, a 48-h culture grown at 37°C in brain heart infusion (BHI) broth (Becton, Dickinson and Company) supplemented with 1% Tween 80 (Sigma-Aldrich) was diluted to ~1 × 10^5 cells/mL in cation-

adjusted Müller-Hinton broth, and 100 μL aliquots were dispensed on white 96-well flat bottom plates. The compounds were tested in duplicates (64 - 0.03 μg/mL) in the cell suspension. After incubation with shaking (180 rpm) at 37°C for 48 h, cell viability was determined using the BacTiter-Glo assay (Promega, Germany) according to the manufacturer's instructions, using a LUMIstar OPTIMA microplate luminometer (BMG Labetch, Germany) for read-out. IC_{80} values, defined as the lowest concentration causing ≥80% reduction of the luminescence intensity, were recorded. For determining activity against *M. tuberculosis* H37Rv ATCC 27294, the Microplate Almar Blue Assay (MABA) was performed as described previously,[26] using the detection reagent provided with the CellTiter-Blue assay kit (Promega). Read-out was performed on an EnVision fluorescence microplate reader (PerkinElmer USA).

Cytotoxicity. HepG2 Cells (ATCC HB8065) were seeded in 96-well plates (10.000 cells/well) in a total medium volume of 100 µl per well (DMEM-F12; 1% NEAA; 1% NaPyr; 5% SVF) and pre-incubated for four hours at 37 °C and 5% CO_2. Afterwards, 1 µl of tested compounds was added and incubated for 40 hours at 37 °C and 5% CO_2. Cell viability was assed upon addition of 100 µl of CellTiter-Glo reagent (Promega G7571) following manufacturer instructions. The cytotoxicity testing was performed in duplicates.

ASSOCIATED CONTENT

Supporting Information. 1D and 2D NMR spectra and data for **1**-**7**, and (3*R*,5*S*)-5-chloropiperazic acid, together with computational details of **1**. This material is available free of charge via the Internet at http://pubs.acs.org.

AUTHOR INFORMATION

Corresponding Author

*E-mail: Alberto.Plaza@merckgroup.com

Present Addresses

[±] Consumer Health, Research and Development, Merck Selbstmedikation GmbH, Frankfurter Straße 250, 64293 Darmstadt, Germany.

Author Contributions

The manuscript was written through contributions of all authors

Funding Sources

This work was funded by the Hessen State Ministry of Higher Education, Research and the Arts (HMWK) via the LOEWE Center for Insect Biotechnology and Bioresources.

Notes

The authors declare no competing financial interest.

ACKNOWLEDGMENT

We thank Dr. Luigi Totti and Damir Druzinec for facilitating strain fermentations.

REFERENCES

(1) Walsh, C. T.; Wencewicz, T. A. *J. Antibiot.* **2014**, *67*, 7-22.

(2) Newman, D. J.; Cragg, G. M. *J. Nat. Prods.* **2016**, *79*, 629-661.

(3) Izawa, S.; Akutsu, H.; Atomi, T.; Kawabata, S.; Sasaki, K. *J. Antibiot.* **1978**, *31*, 729-731.

(4) (a) Pohanka, A.; Menkis, A.; Levenfors, J.; Broverg, A. *J. Nat. Prod.* **2006**, *69*, 1776-1781.

(b) Konishi, M.; Ohkuma, H.; Sakai, F.; Tsuno, T.; Koshiyama, H.; Naito, T.; Kawaguchi, H. *J.*

Antibiot. **1981**, *34*, 148-159. (c) Lingham, R. B.; Hsu, A. H.; O'Brien, J. A.; Sigmund, J. M.; Sanchez, M.; Gagliardi, M. M.; Heimbuch, B. K.; Genilloud, O.; Martin, I.; Diez, M. T.; Hirsch, C. F.; Zink, D. L.; Liesch, J. M.; Koch, G. E.; Gartner, S. E.; Garrity, G. M.; Tsou, N. N.; Salituro, G. M. *J. Antibiot.* **1996**, *49*, 253-259.

(5) Miller, E. D.; Kauffman, C. A; Jensen, P. R.; Fenical, W. *J. Org. Chem.* **2007**, *72*, 323-330.

(6) Sit, C. S.; Ruzzini, A. C.; Van Aenam, E. B.; Ramadhar, T. R.; Currie, C. R.; Clardy, J. *Proc. Natl. Acad. Sci. U.S.A.* **2015**, *43*, 13150-13154.

(7) (a) Fujii, K.; Ikai, Y.; Oka, H.; Suzuki, M.; Harada, K. I. *Anal. Chem.* **1997**, *69*, 5146–5151. (b) Fujii, K.; Ikai, Y.; Mayumi, T.; Oka, H.; Suzuki, M.; Harada, K. I. *Anal. Chem.* **1997**, *69*, 3346-3352.

(8) Cai, G.; Napolitano, J. G.; McAlpine, J. B.; Wang, Y.; Jaki, B. U.; Suh, J.-W.; Yang, S. H.; Lee, I. A.; Franzblau, S. G.; Pauli, G. F. Cho, S. *J. Nat. Prods.* **2013**, *76*, 2009-2018.

(9) (a) Andreou, T.; Costa, A. M.; Esteban, L.; Gonzalez, L.; Mas, G.; Vilarrasa, J. *Org. Lett.* **2005**, *7*, 4083-4086. (b) Manaviazar, S.; Stevenson, P. J.; Hale, K. J..*Tetrahedron Lett.* **2015**, *56*, 3662-3666.

(10) Son, S.; Ko, S.-K.; Jang, M.; Lee, J. K.; Ryoo, I.-J.; Lee, J.-S.; Lee, K. H.; Soung, N.-K.; Oh, H.; Hong, Y.-S.; Kim, B. Y.; Jang, J.-H.; Ahn, J. S. *Org. Lett.* **2015**, *17*, 4046-4049.

(11) Xi, N.; Alemany, L. B.; Ciufolini, M. A. *J. Am. Chem. Soc.* **1998**, *120*, 80-86.

(12) Bifulco, G.; Dambruoso, P.; Gomez-Paloma, L.; Riccio, R. *Chem. Rev.* **2007**, *107*, 3744-3779.

(13) Di Micco, S.; Zampella, A.; D'Auria, M. V.; Festa, C.; De Marino, S.; Riccio, R.; Butts, C. P.; Bifulco, G. *Beilstein J. Org. Chem.*, **2013**, *9*, 2940–2949.

(14) Grimblat, N.; Zanardi, M. M.; Sarotti, A. M. *J. Org. Chem.* **2015**, *80*, 12526-12534.

(15) (a) Oelke, A. J.; France, D. J.; Hofmann, T.; Wuitschike, V.; Ley, S. V. *Nat. Prod. Rep.* **2011**, *28*, 1445-1471. (b) Handy, E. L.; Totaro, K. A.; Lin, C. P.; Sello, J. K. *Org. Lett.* **2014**, *16*, 3488-3491.

(16) Reed, K. A.; Manam, R. R.; Mitchell, S. S.; Xu, J.; Teisan, S.; Chao, T.-H.; Deyanat-Yadzi, G.; Neuteboom, S. T. C.; Lam, K. S.; Potts, B. C. M. *J. Nat. Prod.* **2007**, *70*, 269-276.

(17) Neumann, C. S.; Jiang, W.; Heemstra, J. R., Jr.; Gontang, E. A.; Kolter, R.; Walsh, C. T. *ChemBioChem* **2012**, *13*, 972-976.

(18) Huang, X.; Roemer, E.; Sattler, I.; Moellmann, U.; Christner, A.; Grabley, S. *Angew. Chem. Int. Ed.* **2006**, *45*, 3067-3072.

(19) Maestro 10.2; Schrödinger, *LLC: New York*, NY, **2015**.

(20) MacroModel, 10.2; Schrödinger *LLC New York,* NY, **2013**.

(21) Frisch, M. J. T.; G. W.; Schlegel, H. B.; Scuseria, G. E.; Robb, M. A.; Cheeseman, J. R.; Scalmani, G.; Barone, V.; Mennucci, B.; Petersson, G. A.; Nakatsuji, H.; Caricato, M.; Li, X.; Hratchian, H. P.; Izmaylov, A. F.; Bloino, J.; Zheng, G.; Sonnenberg, J. L.; Hada, M.; Ehara, M.; Toyota, K.; Fukuda, R.; Hasegawa, J.; Ishida, M.; Nakajima, T.; Honda, Y.; Kitao, O.; Nakai, H.; Vreven, T.; Montgomery, J. A., Jr.; Peralta, J. E.; Ogliaro, F.; Bearpark, M.; Heyd, J. J.; Brothers, E.; Kudin, K. N.; Staroverov, V. N.; Kobayashi, R.; Normand, J.; Raghavachari, K.; Rendell, A.; Burant, J. C.; Iyengar, S. S.; Tomasi, J.; Cossi, M.; Rega, N.; Millam, J. M.; Klene,

M.; Knox, J. E.; Cross, J. B.; Bakken, V.; Adamo, C.; Jaramillo, J.; Gomperts, R.; Stratmann, R. E.; Yazyev, O.; Austin, A. J.; Cammi, R.; Pomelli, C.; Ochterski, J. W.; Martin, R. L.; Morokuma, K.; Zakrzewski, V. G.; Voth, G. A.; Salvador, P.; Dannenberg, J. J.; Dapprich, S.; Daniels, A. D.; Farkas, Ö.; Foresman, J. B.; Ortiz, J. V.; Cioslowski, J.; Fox, D. J. *Gaussian 09, Revision A.02*, Gaussian, Inc., Wallingford CT, **2009**.

(22) Cimino, P.; Gomez-Paloma, L.; Duca, D.; Riccio, R.; Bifulco, G. *Magn. Reson. Chem.* **2004**, *42*, 26-33.

(23) Tomasi, J.; Mennucci, B.; Cammi, R. *Chem. Rev.* **2005**, *105*, 2999-3093.

(24) Sarotti, A. M.; Pellegrinet, S. C. *J. Org. Chem.* **2009**, *74*, 7254-7260.

(25) Sarotti, A. M.; Pellegrinet, S. C. *J. Org. Chem.* **2012**, *77*, 6059-6065.

(26) Collins, L.; Franzblau, S. G. *Antimicrob. Agents Chemother.* **1997**, *41*, 1004-1009.